



International Journal of Innovative Research in Computer and Communication Engineering

(A High Impact Factor, Monthly, Peer Reviewed Journal)

Vol. 4, Issue 6, June 2016

Impact of Energy Storage on Hybrid Ac-Dc Micro-grid During Pulse Load

D.Lakshmidurga

Assistant Professor, Department Of EEE, Indo American Institutions Technical Campus, Visakhapatnam, India.

ABSTRACT: Renewable energy based distributed generation plays an important role in electricity production. Electricity is consumed at the same time as it is generated. In this paper, a hybrid AC-DC Micro-grid is considered in islanding mode with solar energy; energy storage is proposed for integration of a pulse load. A synchronous generator is used to connect to the AC side. The AC and DC sides are linked through a bidirectional AC-DC inverter in order to control the power flow between AC and DC sides of the system. When a pulsed load is connected or disconnected on the AC side, the AC side voltage and frequency are maintained within limits by the support of energy storage on DC. Simulation results show that the proposed micro-grid with control algorithms has maintained a balanced current and voltage profile thereby improving the system reliability and stability.

KEYWORDS: Energy storage, grid control, hybrid micro-grid, solar PV system, voltage and frequency amplitude regulation, mat lab.

INTRODUCTION

Now-a-days power system network has become more complex and it has to provide secure, reliable and quality energy of supply to the communities. Reliability and stability of a power system can be improved by introducing the concept of micro-grid. Micro-grid is formed by integrating renewable energy sources into the distribution systems.

Renewable energy based distributed generation plays an important role in electricity production. Electricity is consumed at the same time as it is generated. The amount of electricity must always be provided to meet the varying load demands. An imbalance between supply and demand will damage the stability and quality (voltage and frequency) of the power supply even when it does not lead to unsatisfied demand. Renewable energy such as solar, have some drawbacks like renewable energy load intermittenencies and load mismatches. In order to by-pass these constraints, the concept of photovoltaic systems integrated with an energy storage to match the supply and demand of energy is essential for large-and small-scale applications.

In this paper, a hybrid AC-DC micro-grid with solar energy, energy storage (battery), and a pulse load is proposed. By utilizing sustainable energy and influencing pulse load, the micro-grid can be viewed as a PEV parking garage power system or a ship's power system. Solar panel connected to the AC bus through boost converter and battery banks inject or absorb energy on DC bus to regulate the DC side voltage. The frequency and voltage of the AC side are regulated by a bidirectional AC-DC inverter. The power control of these devices serves to increase the system stability and reliability. This paper is organised as follows: single line diagram of micro-grid system and its components are presented in section II. Coordinated control of converter in islanding mode is presented in section III. Section IV demonstrates the simulation results that verify the proposed topology and control method that increase the system stability under the influence of a pulse load. Finally conclusions are drawing in section V.

II. SINGLE LINE DIAGRAM OF MICRO-GRID SYSTEM AND ITS COMPONENTS

Figure1 represents the Hybrid Micro-grid configuration where various AC, DC sources and loads are connected to corresponding AC and DC networks. The AC and DC sides are linked through a bidirectional three phase AC-DC inverter and transformer. The various characteristics and the component used in the hybrid Micro-grid system are depending on the application.

International Journal of Innovative Research in Computer and Communication Engineering

(A High Impact Factor, Monthly, Peer Reviewed Journal)

Vol. 4, Issue 6, June 2016

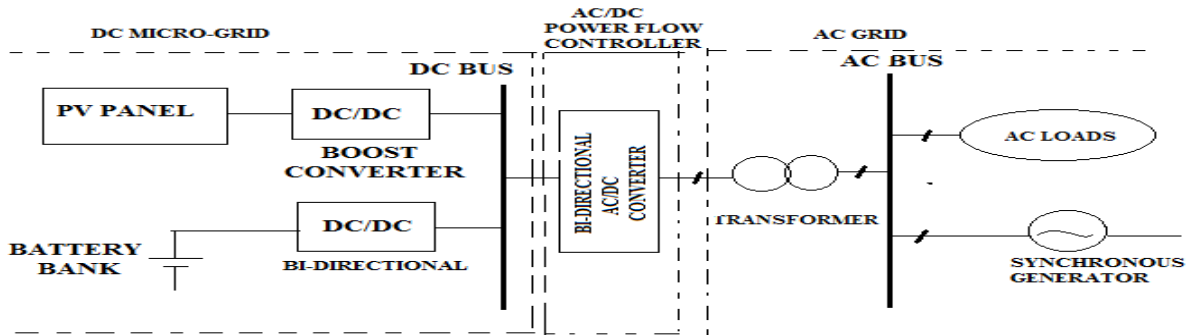


Figure 1: hybrid ac-dc Micro-grid power system.

2.1. Modeling Of Lithium-Ion Battery Bank

An accurate battery cell model is needed to regulate the DC bus voltage in islanding mode. The battery terminal voltage and SOC need to be estimated during operation. A high Fidelity electrical model of lithium-ion battery model with Thermal dependence is used. The equivalent circuit of the Battery model is shown in Figure 2.

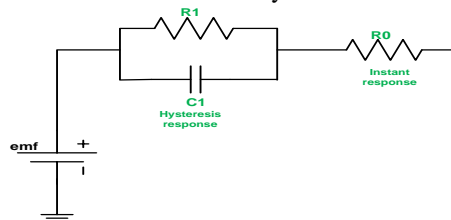


Figure 2: Lithium-ion Battery Equivalent Circuit.

The instantaneous response modeled by a resistor R_0 and the hysteresis response is modeled by a non-linear RC circuit R_1 and C_1 . Emf represents the internal voltage of the battery. All four parameters are varying with different SOC and temperatures, so four lookup tables are established by using the parameter estimation. Tool box in Simulink Design Optimization for these four Parameters under different SOC and temperatures. The flow Diagram of the parameter estimation procedure is shown in Figure 3.

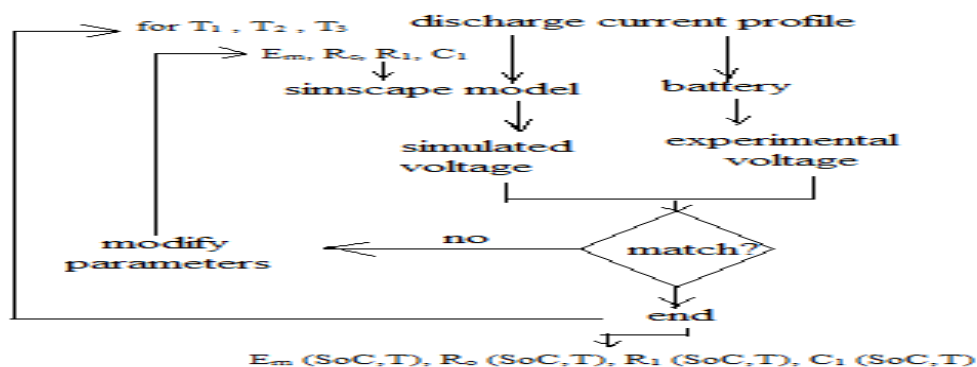


Figure 3: Flow Diagram of the Parameter Estimation Procedure.

The SOC of each single battery cell can be calculated by equation (1).

$$SOC = 100(1 + \frac{\int i_b dt}{Q}) \text{----- (1)}$$

International Journal of Innovative Research in Computer and Communication Engineering

(A High Impact Factor, Monthly, Peer Reviewed Journal)

Vol. 4, Issue 6, June 2016

2.2. Modeling of PV model

Figure 3 shows the equivalent circuit of PV panel (2)-(7) shows mathematical equations of PV panel and its output current all the parameters are shown in table 1

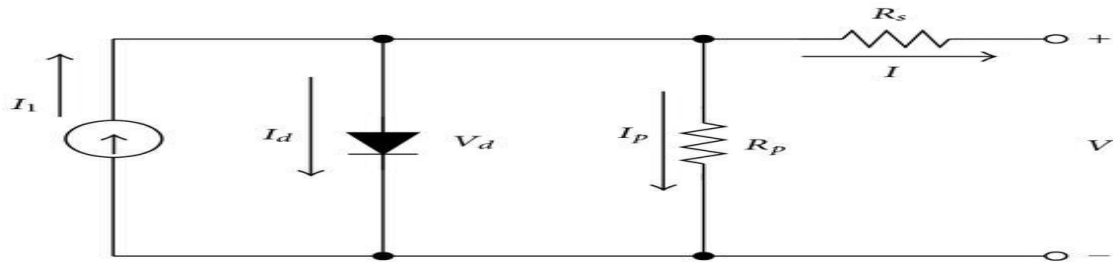


Figure 3: Equivalent PV panel.

Table 1:Parameters for photovoltaic cell.

Symbol	Description	Value
V_{oc}	Rated open circuit voltage	64.2V
I_{ph}	Photocurrent	5.9602 A
I_{sat}	Module reverse saturation current	1.1753×10^{-8}
Q	Electron charge	1.602×10^{-19} C
A	Ideality factor	1.50
K	Boltzman constant	1.38×10^{-23} J/K
R_s	Series resistance of a PV cell	0.037998 Ω
R_p	Parallel resistance of a PV cell	993.51 Ω
I_{sso}	Short-circuit current	5.96 A
K_i	SC current temperature coefficient	1.7×10^{-3}
T_r	Reference temperature	301.18 K
E_{gap}	Energy of the band gap for silicon	1.1 eV
N_p	Number of cells in parallel	528
N_s	Number of cells in series	480
S	Solar radiation level	0~1000 w/m ²
T	Surface temperature of the PV	350 K

$$I_{pv} = n_p I_{ph} - n_p I_{sat} \left[\exp \left(\frac{q}{kT} \left(\frac{V_{pv}}{n_s} + I_{pv} R_s \right) \right) - 1 \right] \text{----- (2)}$$

Where,

$$I_{ph} = (I_{sso} + k_i(T - T_r)) \frac{S}{1000} \text{----- (3)}$$

$$I_{sat} = I_{rr} \left(\frac{T}{T_r} \right)^3 \exp \left(\frac{(qE_{gap})}{kA} \left(\frac{1}{T_r} - \frac{1}{T} \right) \right) \text{---- (4)}$$

$$V_{oc} = n_s \ln \left(\frac{I_{sc}}{I_0} + 1 \right) \left(\frac{AKT_c}{q} \right) \text{----- (5)}$$

$$R_p T = \frac{n_p}{n_s} R_p \text{----- (6)}$$

$$R_s T = \frac{n_s}{n_p} R_s \text{----- (7)}$$

International Journal of Innovative Research in Computer and Communication Engineering

(A High Impact Factor, Monthly, Peer Reviewed Journal)

Vol. 4, Issue 6, June 2016

III. COORDINATED CONTROL OF CONVERTER

Three types of converters are utilized in this proposed hybrid micro grid. These converters must be actively controlled in order to supply uninterrupted power with high efficiency and quality to critical loads on the AC and DC sides during islanding mode. The control method for the converters is discussed in this section.

3.1. Boost Converter Control with MPPT

In islanding mode, the boost converter of the PV farm operates in on-MPPT or off-MPPT which is based on the system's power balance and the SOCs of the battery banks. In most situations, this boost converter can operate in the on-MPPT mode since the variation of the solar irradiance is much slower compared with the power adjustment ability of the AC generator. Therefore, for a given load either on the AC or DC side, the PV should supply as much power as possible to maximize its utilization. However, if the battery banks' SOCs are high (near fully charged) and the PV's maximum output power is larger than the total load in the hybrid microgrid, the PV should be turned to off-MPPT to help the system balance the power flow.

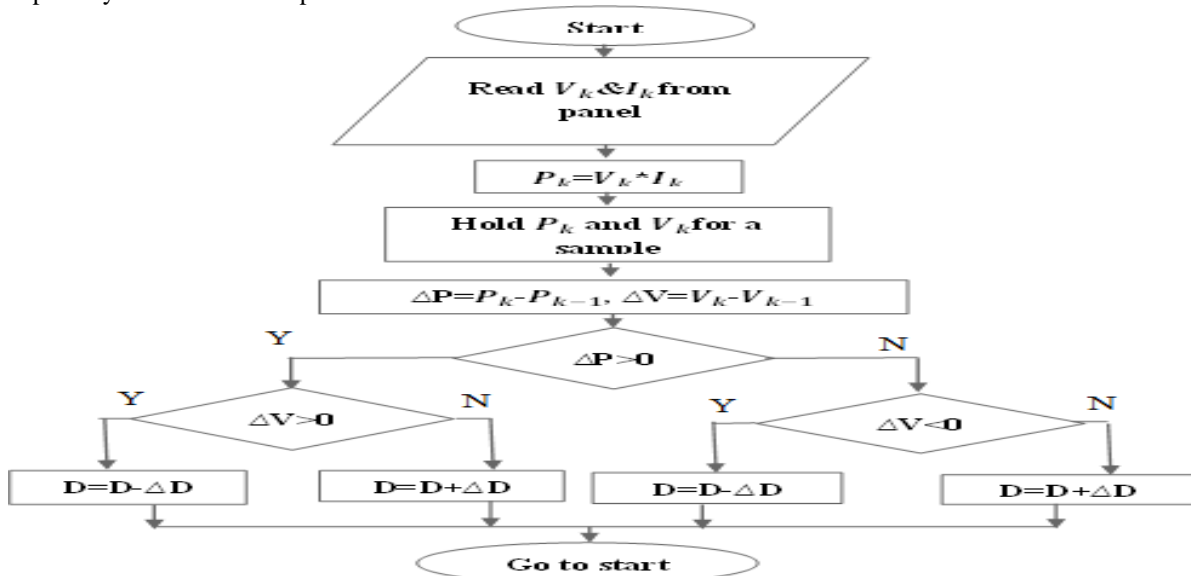


Figure 4: Flow chart of P&O MPPT method.

Shown in fig.4 The algorithm observes output power of the array and perturbs the power based on increment of the array voltage. The algorithm continuously increments or decrements the reference voltage based on the value of the previous power sample. Here a reference voltage V_{ref} is set corresponding to the peak power point of the module. The value of current and voltage can be obtained from the solar PV module. From the measured voltage and current power is calculated. The value of voltage and power at k_{AB} instant are stored. Then values at $[(k+1)]_{AB}$ instant are measured again and power is calculated from the measured values.

3.2. Bi-directional DC-DC converter control

The bi-directional converters of the batteries play an important role in islanding mode to regulate the DC bus voltage. A two closed-loops controller is used to regulate the DC bus voltage. The control scheme for the bi-directional DC-DC converter is shown in fig 5.

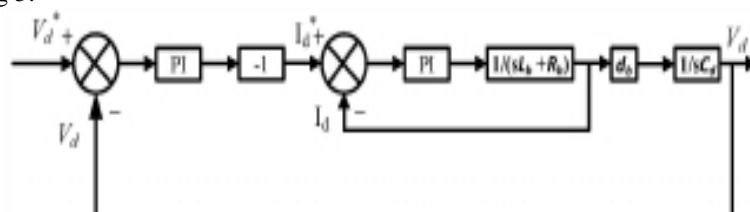


Figure 5: The control block diagram for bi-directional DC-DC converter.

International Journal of Innovative Research in Computer and Communication Engineering

(A High Impact Factor, Monthly, Peer Reviewed Journal)

Vol. 4, Issue 6, June 2016

The outer voltage controlled loop is used to generate a reference charging current for the inner current controlled loop. The error between the measured DC bus voltage and the system reference DC bus voltage is set as the input of the PI controller, and the output is the reference current. The inner current control loop will compare the reference current signal with the measured current flow through the converter and finally generate a PWM signal to drive the IGBT STd or STc to regulate the current flow in the converter. For example, when the DC bus voltage is higher than the reference voltage, the outer voltage controller will generate a negative current reference signal, and the inner current control loop will adjust the duty cycle to force the current flow from the DC bus to the battery, which results in charging of the battery. The energy transfer from DC bus to the battery and the DC bus voltage will decrease to the normal value. If the DC bus voltage is lower than the normal value, the outer voltage control loop will generated a positive current reference signal, which will regulate the current flow from the battery to the DC bus, and because of the extra energy injected from the batteries, the DC bus voltage will increase to the normal value.

3.3. Bi-directional AC-DC inverter control

The frequency and voltage amplitude of the three phase AC side is not fixed during islanding operation so a device is needed to regulate these variables. A bi-directional AC-DC inverter is used with the active and reactive power decoupling technique to keep the AC side stable. The Control scheme for the bi-directional AC-DC inverter is shown in Fig. 8. In d-q co-ordinates, Id is controlled to regulate the active power flow through the inverter to regulate the AC side frequency, and Iq is controlled to regulate the reactive power flow through the inverter to regulate the AC side voltage amplitude.

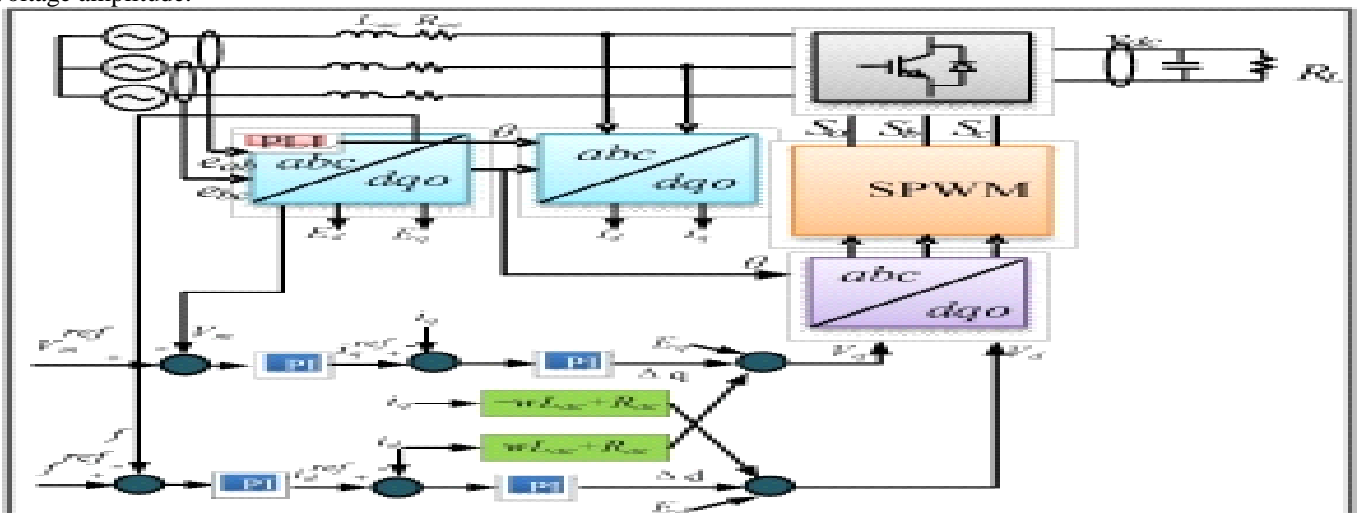


Figure 6: The control block diagram for bi-directional AC-DC converter.

Multi-loop control is applied for both frequency and voltage regulation. For frequency control, the error between measured frequency and reference frequency is sent to a PI controller which generates the id reference. To control the voltage amplitude, the error between the measured voltage amplitude and the reference voltage amplitude is sent to a PI controller to generate iq reference. Equations (8) show the AC side voltage equations of the bi-directional AC-DC inverter in ABC and d-q coordinates respectively. Where (Va, Vb, Vc) are AC side voltages of the inverter, and (Ea, Eb, Ec) are the voltages of the AC bus.

$$L_{ac} \frac{d}{dt} \begin{bmatrix} i_a \\ i_b \\ i_c \end{bmatrix} + R_{ac} \begin{bmatrix} i_a \\ i_b \\ i_c \end{bmatrix} = \begin{bmatrix} V_a \\ V_b \\ V_c \end{bmatrix} - \begin{bmatrix} E_a \\ E_b \\ E_c \end{bmatrix} + \begin{bmatrix} \Delta_a \\ \Delta_b \\ \Delta_c \end{bmatrix} \dots \dots \dots (8)$$

When the pulse load is connected or disconnected to the AC side, the frequency or the voltage amplitude will be altered. After detecting the variance from the phase lock loop (PLL) or voltage transducer, Id and Iq reference signals will be adjusted to regulate power flow through the bi-directional AC-DC inverter. Because of the power flow variances, the DC bus voltage will also be influenced. The DC bus voltage transistor will sense the voltage variance in the DC bus, and the bi- directional DC-DC converter will regulate the current flow between the battery and the DC bus. In the end, the energy is transferred between the battery and the AC side to balance the power flow in the system.

International Journal of Innovative Research in Computer and Communication Engineering

(A High Impact Factor, Monthly, Peer Reviewed Journal)

Vol. 4, Issue 6, June 2016

IV. SYSTEM SIMULATION RESULTS

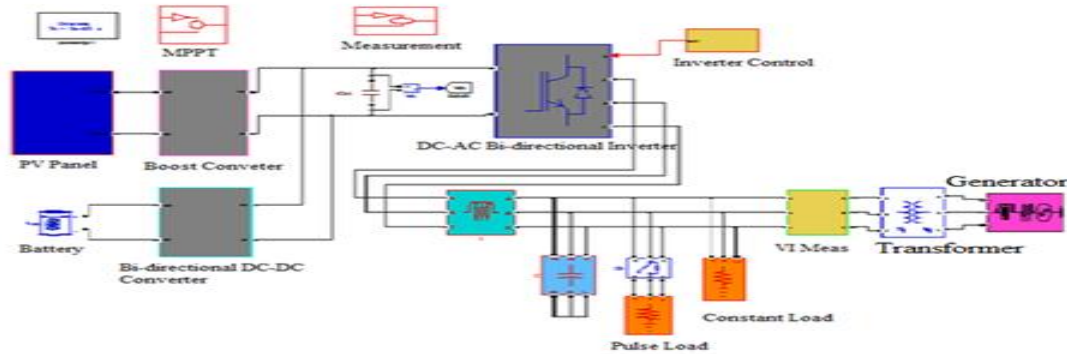


Figure 7: MATLAB/SIMULINK of hybrid AC-DC Micro-Grid with solar energy, energy storage and critical load.

The operation of the hybrid micro grid utilizing a 10.07kw PV farm under the influence of a 10kw pulse load is simulated to verify the proposed control algorithms. The rated output power of the synchronous generator is 13.8kw, and a 4kw constant load is connected in the AC side. Five 51.8v 21Ah Lithium-ion battery banks are connected individually to the DC bus through bidirectional DC-DC converters. The system parameters for the Micro-grid are listed in table II.

Table II: Hybrid Micro-grid System Parameters.

Symbol	Description	Value
C_{pv}	Solar panel capacitor	100 μ F
L_{pv}	Inductor for solar panel boost converter	5mH
C_d	DC bus capacitor	6000 μ F
L_{ac}	AC filter inductor	1.2 mH
R_{ac}	Inverter equivalent resistance	0.3 Ω
L_b	Battery converter inductor	3.3 mH
R_b	Resistance of L_b	0.5 Ω
F	Rated AC grid frequency	60Hz
V_d	Rated DC bus voltage	300V
V_m	Rated AC bus p-p voltage (rms)	8V
$n1/n2$	Transformer ratio	1:1
	AC side load	14KW

Figure 8 shows PV farm power control with MPPT. The output power, the terminal voltage, current of the PV panel, the duty cycle of the boost converter and the solar irradiance.

Two kinds of solar irradiance variances with different charging rates are used in this study. Before 0.4s, the duty cycle is set at 0.5s, the terminal voltage of the PV panel is 149v and the output power from the PV panel is only 9.56kw, after the MPPT is enabled, the duty cycle is decreased to 0.45. And the terminal voltage is increased to 165V. In this way, the PV panel reaches the maximum power output of 10.07kw. The simulation results show that the boost converter with MPPT functionality can track the maximum power point with fast response.

When the 10kw resistive pulse load was connected to the AC bus, the total load in the AC side was 14kw, and 13.8kw generation of generator was connected to the AC side. Which exceeded the generator's output limitation by 0.2kw without energy storage device condition.

International Journal of Innovative Research in Computer and Communication Engineering

(A High Impact Factor, Monthly, Peer Reviewed Journal)

Vol. 4, Issue 6, June 2016

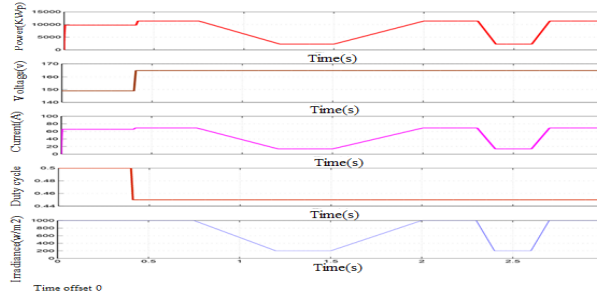


Figure 8: PV farm output power control with MPPT.

Fig. 9 represents AC bus voltage with pulse load influence. When $t=2s$ the pulse load is connected to the system, before 2s generation in the AC side delivers to the system but when pulse load is connected to the system, the generation in the AC side is not sufficient to the total load so at $t=2.2s$, the system collapsed, and voltage dropped considerably. The system couldn't recover even after the pulse load was disconnected after $t=3s$

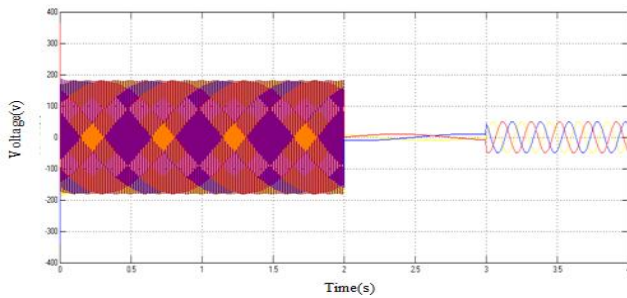


Figure 9: AC bus voltage with pulse load influence.

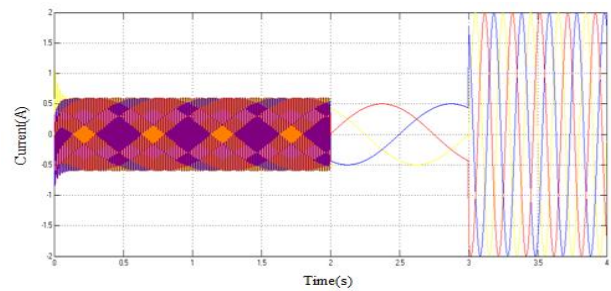


Figure 10: AC bus current with AC pulse load influence.

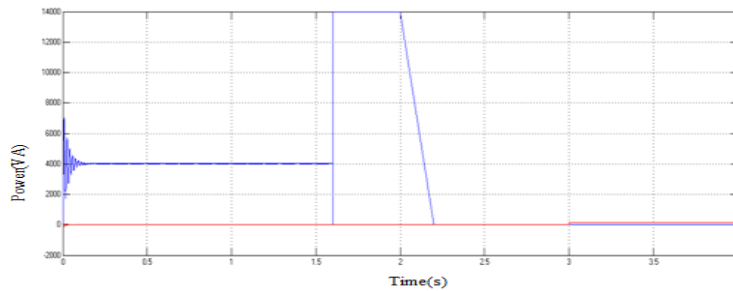


Figure 11: Micro-grid AC side pulse load response without DC support.

with AC pulse load influence. The AC side current without DC side aid by the AC-DC inverter. At $t=2.2s$, the system collapsed, current raised suddenly, the system couldn't recover even after the pulse load was disconnected after $t=3s$. The batteries are able to support the AC side by injecting or absorbing power to the AC bus through the bidirectional inverter that links the AC and DC side. The frequency and voltage amplitude on the AC side also remain stable due to the separate control of the active and reactive power flow control.

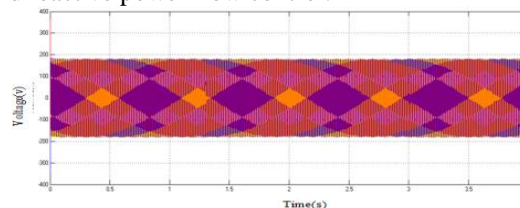


Figure 12: Micro-grid AC side voltage and current response with DC support.

International Journal of Innovative Research in Computer and Communication Engineering

(A High Impact Factor, Monthly, Peer Reviewed Journal)

Vol. 4, Issue 6, June 2016

The AC bus voltage transient response during the pulse load variation is shown in Fig. 12. When pulse load is connected and disconnected for a particular time intervals to the system, the AC voltage amplitude returned to its normal value in less than three cycles.

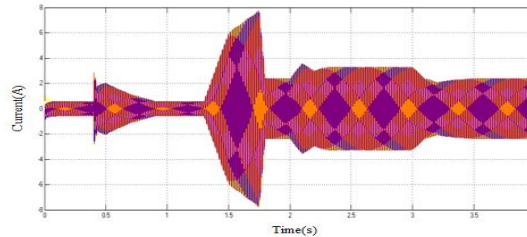


Figure 13: AC side current with AC pulse load influence.

Figure 13 shows AC side current with pulse load influence. When the pulse load is connected to the AC side, the current flow through the AC bus increased immediately, and after the pulse load disconnected from the AC side, the current slightly decreased to keep the system in balanced.

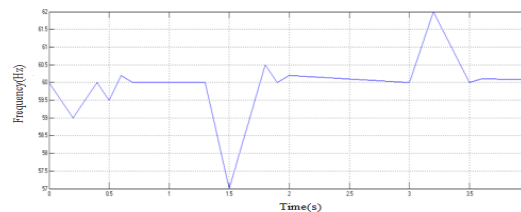


Figure 14: AC side frequency response.

Figure 14 shows the AC side frequency variation. The AC-DC bi-directional inverter was enabled at $t=0.4s$, and the AC side frequency was stable at 60 HZ in less than 0.4s. When the resistive pulse load is connected at $t=1.3s$, the frequency dropped to 57Hz and returned to 60Hz in less than one second. When the pulse load was disconnected from the AC side, the frequency increased to 62Hz and returned to steady state in less than 0.5s.

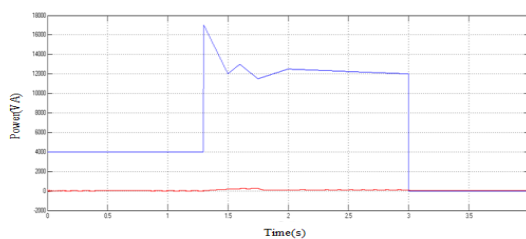


Figure 15: Generator output active and reactive power.

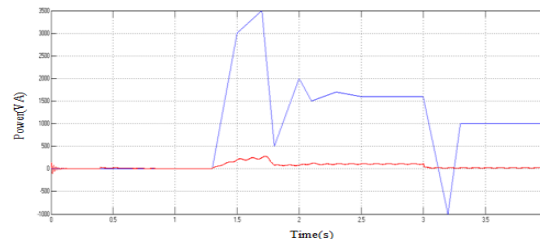


Figure 16: AC bus power flow with AC side pulse load.

The power flow through the AC bus and the power generated from the generator is shown in Fig. 15, 16. The hybrid micro grid is stable in both its AC and DC side.

V. CONCLUSION

In this thesis work, the proposed hybrid AC-DC Micro-grid operated in islanding mode. The Micro-grid has a PV farm and synchronous generator supply energy to its DC and AC side. Battery banks are connected to the DC bus through bi-directional DC-DC converter. By using above combinations it can be stated that the load demand is optimally met by using proposed hybrid system and the excess electricity is reduced by integration of batteries. By using above system i.e., Micro-grid power system without battery support the system is not stable, whereas micro-grid power system with battery support the system is stable under the influence of pulse load. The AC side voltage amplitude and frequency are regulated by the bi-directional AC-DC inverter. This also provides reliably to the system by having more generation with the inclusion of renewable sources along with generator. Hence, the reliability of the system is increased with the inclusion of batteries into the system.



International Journal of Innovative Research in Computer and Communication Engineering

(A High Impact Factor, Monthly, Peer Reviewed Journal)

Vol. 4, Issue 6, June 2016

REFERENCES

1. CK Sao, PW Lehn, Control and power management of converter fed MicroGrids, IEEE Trans. Power Syst., 2008; 23: 1088-1098.
2. A Mohamed, F Carlos, et al. Operation and protection of photovoltaic systems in hybrid AC/DC smart grids, IECON 2012 - 38th Annual Conference on IEEE Industrial Electronics Society, 2012; 11 04-11 09.
3. RH Lasseter, P Paigi, Micro-grid: A conceptual solution, in Proc.IEEE 35th PESC, 2004; 6: 4285--4290.
4. SX Chen, HB Gooi, et al. Sizing of energy storage for Micro-Grids, IEEE Transactions on smart grid, March 2012; 3.
5. Klaus Jäger, Olindo Isabella, et al. Solar Energy: Fundamentals, technology, and systems, Delft University of technology, 2014.
6. DVN Ananth, performance evaluation of solar PV system using maximum power point tracking algorithm with battery backup, internal conference 2011.
7. David Linden, Thomas B Reddy, Handbook of batteries, third edition, McGraw-Hill, 1995.
8. Robyn A. Jackey, A simple, effective lead-acid battery modeling process for electrical system component selection, the Mathworks, inc.
9. Gagari Deb, Ramanandapaul, et al. Hybrid power generation system, international journal of computer and electrical engineering, 2012; 4.
10. A Sannino, G Postiglione, et al. Feasibility of a DC network for commercial facilities," IEEE Trans. Ind. Appl., sep.2003; 39: 1409-1507.
11. S Bose, Y Liu, et al. Tie line Controls in Micro-grid Applications, in iREP Symposium Bulk Power System Dynamics and Control VII, Revitalizing Operational Reliability, Aug. 2007; 1-9.